arXiv:1202.2787v2 [hep-lat] 16 Feb 2012

The $\pi\pi$ Interaction in the ρ Channel in Finite Volume

Hua-Xing Chen[1,2*] and E. Oset[1†]
[1] *Departamento de Física Teórica and IFIC, Centro Mixto Universidad de Valencia-CSIC, Institutos de Investigación de Paterna, Aptdo. 22085, 46071 Valencia, Spain*
[2] *School of Physics and Nuclear Energy Engineering, Beihang University, Beijing 100191, China*

(Dated: February 17, 2012)

We evaluate the levels of the $\pi\pi$ system in the ρ channel in finite volume. We investigate the dependence on the π mass and compare with other approaches which use QCD lattice calculations and effective theories. We also illustrate the errors induced by using the conventional Lüscher approach instead of a more accurate one recently developed that takes into account exactly the relativistic two meson propagators. Finally we make use of this latter approach to solve the inverse problem, getting $\pi\pi$ phase shifts from "synthetic" lattice data and show which accuracy is needed in these data to obtain the ρ properties with a desired accuracy.

PACS numbers: 11.80.Gw, 12.38.Gc, 12.39.Fe, 13.75.Lb

I. INTRODUCTION

The determination of hadron spectra is one of the challenging tasks of Lattice QCD and many efforts are being devoted to this problem [1–19]. As one is aiming at higher accuracy and consistency with the decay channels of the hadrons, Lüscher's approach [20, 21], reconstructing phase shifts of the decay products from the discrete energy levels of the box, is playing gradually a more important role. Other strategies formerly used, like making use of the "avoided level crossing", are leaving room to other methods once this criteria has been shown insufficient for resonances with a large width [22–24].

One of the hadrons that has received more attention is the ρ meson. There have been a few attempts to describe the ρ using Lüscher's approach [25–30]. On the other hand the first lattice estimate of the $\rho \to \pi\pi$ amplitude [31] did not apply Lüscher's method. The most recent work on the ρ properties from the lattice point of view is the one of [18] and we shall refer to it for comparison along the paper. In between in [24] Lüscher's approach has been recently simplified and improved by keeping the full relativistic two body propagator (Lüscher's approach keeps the imaginary part of this propagator exactly but makes approximations on the real part) and extending the method to two or more coupled channels. The method has also been applied in [32] to obtain finite volume results from the Jülich model for meson baryon interaction and in [33], to study the interaction of the DK and ηD_s system where the $D_{s^*0}(2317)$ resonance is dynamically generated from the interaction of these particles [34–37]. The case of the κ resonance in the $K\pi$ channel is also addressed along the lines of [24] in [38] and an extension of the approach of [24] to the case of interaction of unstable particles has been made in [39].

In the present work we shall use the approach of [24] to the case of the interaction of two pions in p-waves and isospin $I = 1$, the ρ channel. On the first part we shall use the chiral unitary approach to $\pi\pi$ scattering in p-waves from [40, 41] and apply it to get energy levels in a finite box. We shall then see how they change with the pion mass to establish connection with lattice results which run for heavier masses than the physical pion mass. In a second step we will face the inverse problem of getting $\pi\pi$ phase shifts from the energy spectra in the box, determining the precision needed in the lattice spectra to get the phase shifts with a demanded accuracy.

II. FORMALISM OF THE CHIRAL UNITARY APPROACH FOR THE ρ IN INFINITE AND FINITE VOLUME.

We shall follow here the approach of [41] to get the $\pi\pi$ scattering amplitude in p-waves. In this work the pion and kaon form factors were studied using the chiral Lagrangians of [42] and those for the coupling of resonances to pairs of pseudoscalar mesons of [43]. The work was done obtaining a kernel, or $\pi\pi$ potential, from those Lagrangians, which contains a contact term from the lowest order Lagrangian of [42] and another term, the explicit ρ pole, with the

---

[*] Electronic address: hxchen@ific.uv.es
[†] Electronic address: oset@ific.uv.es

coupling of the ρ to the pions obtained from [43]. One includes also the $K\bar{K}$ system and unitarizes the two channel problem using the coupled channels Bethe Salpeter equations, or the equivalent N/D method. Although one can approach the problem from different perspectives, like the inverse amplitude method (IAM) [44, 45], or the Bethe Salpeter equations with an energy dependent potential provided by the first and second order terms of the chiral Lagrangians of [42], as done in [46], the approach of [41] by separating the contact term and a bare ρ pole, already accepts from the beginning the proven fact that the ρ is not a $\pi\pi$ resonance, but rather a genuine state which has $\pi\pi$ as decay channel. This has been checked thoroughly by looking at the large N_c behaviour of the pole position in [47, 48], where the mass of the ρ stays constant as N_c grows and the width decreases. This is opposite to the composite states, dynamically generated by the interaction, like the light scalar mesons, where the width grows considerably as N_c increases. A different perspective is provided in [49], where it is shown that all chiral logarithms cancel out in the rho-channel, while they do not cancel for the sigma case, and they strongly influence the properties of this latter resonance. In other words, the loops from intermediate $\pi\pi$ states are very relevant for the sigma and highly unimportant for the ρ case. In even simpler words we could say that the sigma is a $\pi\pi$ resonance, while the ρ is a non $\pi\pi$ state which decays in this channel. One way to take this into account is to allow for a CDD (Castillejo, Dalitz, Dyson) pole in the potential [50], and this is what naturally appears by combining the Lagrangians of [42] and [43] and is implemented in the approach of [41].

In the chiral unitary approach one uses the coupled channel Bethe-Salpeter equations in their on shell factorized form [51, 52]

$$\mathbf{T} = (1 - \mathbf{V}\mathbf{G})^{-1}\mathbf{V}\,. \tag{1}$$

The relevant V-matrices for $\pi\pi$ and $K\bar{K}$ scattering have been studied in Ref. [41]:

$$\begin{aligned}
V^{I=1}_{\pi\pi,\pi\pi} &= T_{\pi^+\pi^-,\pi^+\pi^-} = -\frac{2p_\pi^2}{3f^2}\Big(1+\frac{2G_V^2}{f^2}\frac{s}{M_\rho^2-s}\Big)\,,\\
V^{I=1}_{\pi\pi,K\bar{K}} &= \sqrt{2}T_{\pi^+\pi^-,K^+K^-} = -\frac{\sqrt{2}p_\pi p_K}{3f^2}\Big(1+\frac{2G_V^2}{f^2}\frac{s}{M_\rho^2-s}\Big)\,,\\
V^{I=1}_{K\bar{K},K\bar{K}} &= T_{K^+K^-,K^+K^-} - T_{K^+K^-,K^0\bar{K}^0} = -\frac{p_K^2}{3f^2}\Big(1+\frac{2G_V^2}{f^2}\frac{s}{M_\rho^2-s}\Big)\,,\\
V^{I=0}_{K\bar{K},K\bar{K}} &= T_{K^+K^-,K^+K^-} + T_{K^+K^-,K^0\bar{K}^0} = -\frac{p_K^2}{3f^2}\Big(3+\frac{2G_V^2}{f^2}\frac{s}{M_\omega^2-s}+\frac{4G_V^2}{f^2}\frac{s}{M_\phi^2-s}\Big)\,.
\end{aligned} \tag{2}$$

We note that these definitions have a minus sign difference with respect to [41] to follow the more standard notation for V and T. We work in the isospin base, where the states are defined as:

$$|\pi\pi\rangle_{I=1} = \frac{1}{2}|\pi^+\pi^- - \pi^-\pi^+\rangle\,, \tag{3}$$

$$|K\bar{K}\rangle_{I=1} = \frac{1}{\sqrt{2}}|K^+K^- - K^0\bar{K}^0\rangle\,, \tag{4}$$

$$|K\bar{K}\rangle_{I=0} = \frac{1}{\sqrt{2}}|K^+K^- + K^0\bar{K}^0\rangle\,. \tag{5}$$

Note the extra $1/\sqrt{2}$ in the normalization of the pions (unitary normalization) which is adopted to account for the identity of the particles in the intermediate states. Since in this paper we study the ρ meson which has isospin $I = 1$, there are only two channels to be considered, $|\pi\pi\rangle_{I=1}$ and $|K\bar{K}\rangle_{I=1}$. For simplicity, we rewrite the V-matrix as $V_{11} = V^{I=1}_{\pi\pi,\pi\pi}$, $V_{22} = V^{I=1}_{K\bar{K},K\bar{K}}$ and $V_{12} = V^{I=1}_{\pi\pi,K\bar{K}}$.

The parameters in Eq. (2) are also taken from Ref. [41], in particular:

$$\begin{aligned}
G_V &= 53\text{MeV}\,,\\
f &= 87.4\text{MeV}\,.
\end{aligned} \tag{6}$$

But for the bare ρ mass M_ρ of Eqs. (2) we choose the value 837.3 MeV, which is slightly larger than the value 829.8 MeV used in Ref. [41]. Doing this, the phase shifts obtained are slightly better compared with the experimental data [53], as shown in Fig. 4 in the next section.

The G-function for the two-meson propagator having masses m and M is defined as

$$G(p^2) = i\int\frac{d^4q}{(2\pi)^4}\frac{1}{q^2-m^2+i\epsilon}\frac{1}{(p-q)^2-M^2+i\epsilon}\,. \tag{7}$$

In Ref. [41] it has been calculated in the continuum space (infinite volume) using dimensional regularization, and the result is:

$$G_i(s) = \frac{1}{16\pi^2}\Big(-2 + d_i + \sigma_i(s) \log \frac{\sigma_i(s)+1}{\sigma_i(s)-1}\Big)\,, \tag{8}$$

where the subindex i refers to the corresponding two-meson state, either $|\pi\pi\rangle_{I=1}$ $(i=1)$ or $|K\bar{K}\rangle_{I=1}$ $(i=2)$, and $\sigma_i(s) = \sqrt{1-4m_i^2/s}$. The parameters d_i are also taken from Ref. [41] which are fitted with the experimental data of $\pi\pi$ P-wave scattering:

$$\begin{aligned} d_1 &= \frac{m_K^2}{m_K^2 - m_\pi^2}\big(\log\frac{m_\pi^2}{\mu^2} + \frac{1}{2}\log\frac{m_K^2}{\mu^2} + \frac{1}{2}\big)\,, \\ d_2 &= \frac{-2m_\pi^2}{m_K^2 - m_\pi^2}\big(\log\frac{m_\pi^2}{\mu^2} + \frac{1}{2}\log\frac{m_K^2}{\mu^2} + \frac{1}{2}\big)\,, \end{aligned} \tag{9}$$

with $\mu = M_\rho$. Eqs. (9) are taken such as to guarantee a perfect matching with the results of chiral perturbation theory for the form factor of [54].

All the above formulae are for the study of the ρ meson in the infinite space. To study the ρ meson in the finite volume, we just need to change the G-function of dimensional regularization (Eq. (8)) by the one which is defined in the finite box of side L. This was deduced in [33] and it is given by $\tilde{G}(s)$, defined through:

$$\tilde{G}(s) - G(s) = \lim_{q_{\max}\to\infty}\Big(\frac{1}{L^3}\sum_{q_i}^{q_{\max}} I(q_i) - \int_{q<q_{\max}}\frac{d^3q}{(2\pi)^3} I(q)\Big)\,. \tag{10}$$

$$I(q_i) = \frac{1}{2\omega_1(\vec{q})\omega_2(\vec{q})}\frac{\omega_1(\vec{q})+\omega_2(\vec{q})}{E^2 - (\omega_1(\vec{q})+\omega_2(\vec{q}))^2}\,, \tag{11}$$

where $\omega_{1,2}(\vec{q}) = \sqrt{m_{1,2}^2 + \vec{q}^{\,2}}$ and the discrete momenta in the sum given by $\vec{q} = \frac{2\pi}{L}\vec{n}$ $(\vec{n} \in \mathcal{Z}^3)$. In this way we have just changed the integration over momenta by a sum over the discrete values of the momenta allowed by the periodic conditions in the box.

The real part of $\tilde{G}(s) - G(s)$ is shown in Fig. 1 as a function of $q_{\max}$. We note that we have fixed L to be 2.5 m_π^{-1} and E to be 770 MeV. We find that it has a good convergence when one goes to large values of q_{max}. However, as already done in [24, 33] it is more practical and equally accurate to make an average of this quantity for smaller values of q_{max} with the consequent economy in computation.

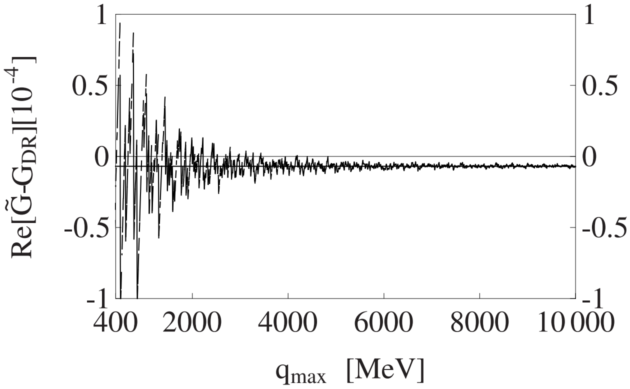

FIG. 1: The difference between $\tilde{G}(s)$ and Re$[G_{\rm DR}(s)]$ calculated using Eq. (10) as a function of $q_{\max}$. Here we choose $L = 2.5\, m_\pi^{-1}$ and E = 770 MeV.

III. THE ENERGY LEVELS IN THE CHIRAL UNITARY APPROACH

Using the $\tilde{G}$-function in Eq. (10), we calculate the energy levels in the finite volume for different values of L, by looking at the poles of the T matrix, which appear when the determinant of $1 - \mathbf{VG}$ is zero:

$$\mathrm{Det}(1-\mathbf{VG}) = 1 - V_{11}\tilde{G}_1(s) - V_{22}\tilde{G}_2(s) + (V_{11}V_{22} - V_{12}^2)\tilde{G}_1(s)\tilde{G}_2(s) = 0\,. \tag{12}$$

As we have said before, our procedure follows closely the method used in Refs. [24, 33, 38, 55], so here we go directly to the discussion of the numerical results. The energy levels for $\pi\pi$ P-wave scattering are functions of the cubic box size L, as well as the pion mass m_π. We shall study the dependence on these variables. The volume dependence is shown here and the pion mass dependence in the next section.

In the left panel of Fig. 2 we show the energy levels as function of L for the coupled channels which are obtained after performing an average for different $q_{\rm max}$ values between 1200 MeV and 2000 MeV. On the right panel we show the same ones separately for values of $q_{\rm max}$ = 1300, 1500, 1700 and 1900 MeV. We find that the energy levels for different $q_{\rm max}$ are almost the same. At least we can not differentiate them in Fig. 2. This surprising result is simply a consequence of the fact that the ρ meson is very weakly tied to the $\pi\pi$ loops, accounted for by the $\tilde{G}$ function, where the L dependence appears. We note that the higher curves seem to cross each other. This does not happen because of the ordering chosen for the levels and then produces the "avoided level crossing", but they are a consequence of the couple channel dynamics. To see it clearly, we show the results for single $\pi\pi$ and $K\bar{K}$ channels in Fig. 3.

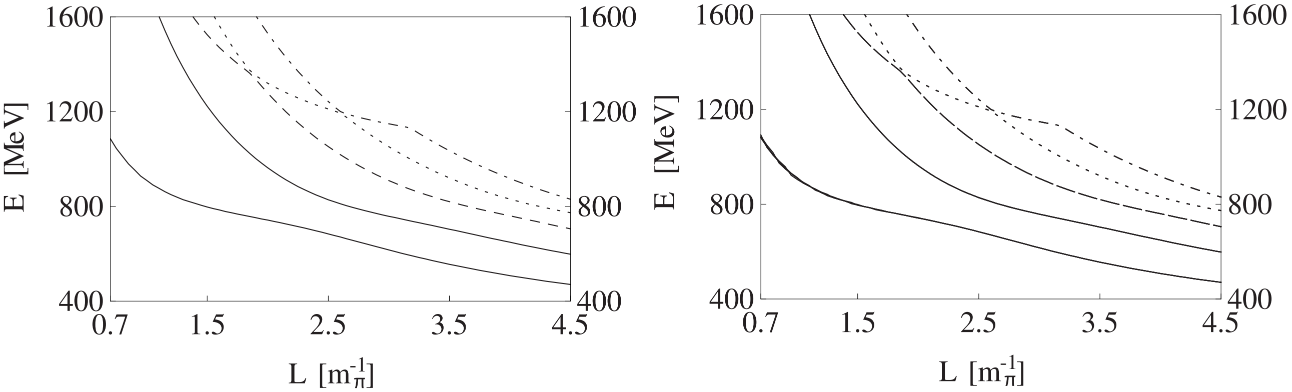

FIG. 2: Energy levels as functions of the cubic box size L, derived from the coupled channels unitary approach of Ref. [41] and using $\tilde{G}$ from Eq. (10). We perform an average for different $q_{\rm max}$ values between 1200 MeV and 2000 MeV in the left figure, while show them separately in the right figure for different $q_{\rm max}$ = 1300, 1500, 1700 and 1900 MeV, which are almost the same.

In Fig. 3 we show the energy levels for the single channel, either the $\pi\pi$ channel or the $K\bar{K}$ one. We find that the first and second energy levels in the left figure, which are are obtained using only the $\pi\pi$ channel, are quite similar to the results for the coupled channels. However, the higher levels are a mixture of both the $\pi\pi$ and the $K\bar{K}$ channels. This is quite reasonable since the $K\bar{K}$ channel does not contribute much in the low energy region. Since the first (lowest) energy level should be well calculated using the chiral unitary approach which is very accurate in this energy region, in the following discussions we shall mainly concentrate on it, and consequently some of our calculations will be done only in the $\pi\pi$ channel.

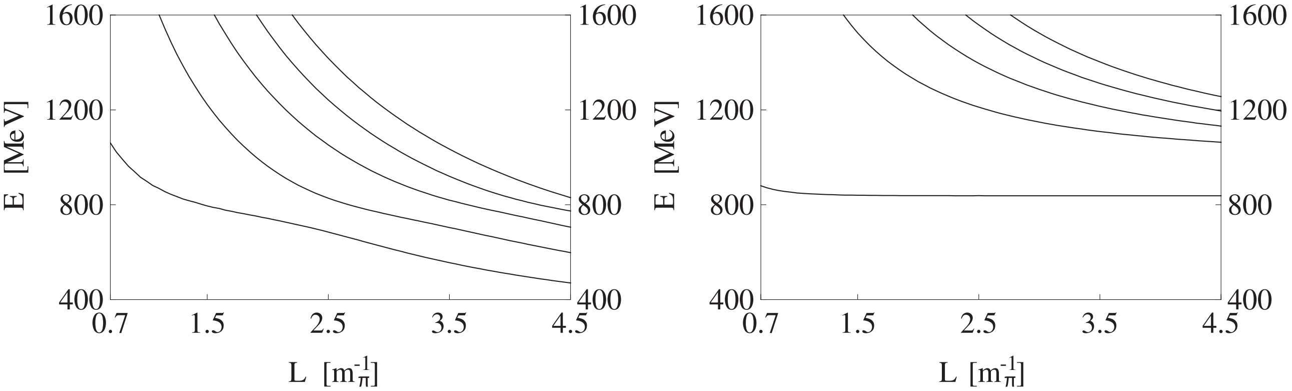

FIG. 3: Energy levels as functions of the cubic box size L for the $\pi\pi$ channel and the $K\bar{K}$ channels, shown in the left and right hand sides, respectively.

From these energy levels, we can obtain their corresponding phase shifts. To do this we use only the $\pi\pi$ channel and follow the procedures used in Ref. [24]. Since the energy levels are obtained by solving the poles of Eq. (12), they satisfy the following relation:

$$1 - \mathbf{V}\tilde{\mathbf{G}} \xrightarrow{\text{one channel}} V_{11}(E)\big(V_{11}(E)^{-1} - \tilde{G}_{11}(E,L)\big) = 0\,, \tag{13}$$

which can be used to calculate the scattering matrix:

$$T_{11}(E,L) = (V_{11}(E)^{-1} - G_{11}(E))^{-1} = (\tilde{G}_{11}(E,L) - G_{11}(E))^{-1}\,. \tag{14}$$

Since this relation holds for the energy levels shown in Fig. 2 and Fig. 3, L and E are not independent. Moreover when we only consider the first (lowest) energy level, we have $T_{11}(E,L) = T_{11}(E,L(E)) = T_{11}(E)$. From this calculated T matrix one can evaluate the $\pi\pi$ P-wave phase shifts which are related to our T by

$$T_{11}(E) = \frac{-8\pi E}{p_{11}\cot\delta(p) - ip_{11}}\,. \tag{15}$$

In Fig. 4, we show the $\pi\pi$ P-wave phase shifts δ, calculated through three different approaches. The solid curve is taken from Ref. [41] using the chiral unitary approach. This result has a good consistence with the experimental data [53]. The dashed curve is the phase shift extracted from the first energy level of the left figure of Fig. 3 obtained using only the $\pi\pi$ channel. The results are the same as the solid curve. The dotted curve is the phase shift extracted from the first energy level of the left figure of Fig. 2, obtained with the coupled channels but using only $\pi\pi$ in the analysis. We find that there are small differences in the high energy region, which are caused by the $K\bar{K}$ channel.

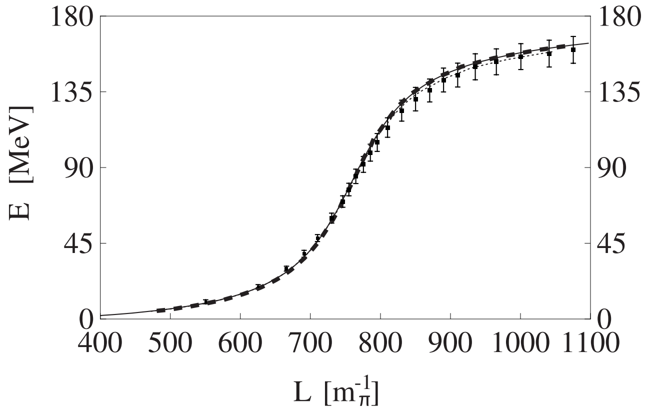

FIG. 4: The solid curve is the $\pi\pi$ scattering P-wave phase shift calculated using the chiral unitary approach [41]. The dashed curve is the phase shift extracted from the first energy level of the left figure of Fig. 3, obtained using only the $\pi\pi$ channel. The dotted curve is the phase shift extracted from the first energy level of the left figure of Fig. 2, obtained using coupled channels.

Using the phase shifts $\delta(E)$ we can fit the physical quantities for the ρ meson, such as m_ρ, $g_{\rho\pi\pi}$ and Γ_ρ. We note that m_ρ is the ρ mass we obtained, i.e., one of our outputs; while M_ρ is the bare ρ mass, i.e., one of our inputs. We use the following two equations to extract the ρ properties:

$$\cot\delta(s) = \frac{m_\rho^2 - s}{\sqrt{s}\Gamma_\rho(s)}\,, \quad \text{and} \quad \Gamma_\rho(s) = \frac{p^3}{s}\frac{g_{\rho\pi\pi}^2}{8\pi}\,. \tag{16}$$

We note that the factor 8π in the second equation is our normalization, while in Ref. [18] the authors use 6π.

The results from fitting the $\pi\pi$ channel (dashed curve shown in Fig. 4) are

$$m_\rho = 768.6 \text{ MeV}\,, g_{\rho\pi\pi} = 6.59\,, \Gamma_\rho = 135 \text{ MeV}\,, \tag{17}$$

while those from fitting the coupled channels (dotted curve shown in Fig. 4) are

$$m_\rho = 769.6 \text{ MeV}\,, g_{\rho\pi\pi} = 6.79\,, \Gamma_\rho = 144 \text{ MeV}\,. \tag{18}$$

This should be compared with the “exact” results with the chiral unitary approach with two channels

$$m_\rho = 767.9 \text{ MeV}\,, g_{\rho\pi\pi} = 6.69\,, \Gamma_\rho = 139 \text{ MeV}\,. \tag{19}$$

It is interesting to show explicitly how the levels appear in this case. As shown in Eq. (13), the energies are obtained for one channel by solving the equation $\left(V_{11}(E)^{-1} - \tilde{G}_{11}(E,L)\right) = 0$. In Fig. 5 we show $V_{11}(E)^{-1}$ and $\tilde{G}_{11}(E,L)$ separately and the points where the two curves cut each other provide the eigenenergies of the box. We observe that $\tilde{G}$ is a small quantity compared with other hadron scattering cases, since it raises very fast close to the poles which are given by the free energies of the box induced by the boundary condition on the sides of the box. The $\pi\pi$ potential is large, and even has a pole, the CDD pole at the bare mass of the ρ. Consequently, $V_{11}(E)^{-1}$ is also a small quantity, passing through zero around the bare ρ mass. The combination of these two facts leads to an eigenenergy of the box with interaction in the vicinity of the bare ρ mass, which defines the first level. For all the other levels the eigenenergies are very close to the free energies and this tells us that they carry small information on the potential. All these features are a consequence of the peculiar nature of the ρ which is not dynamically generated by the interaction of the two pions and cannot be described as a scattering resonance from an ordinary potential, but is a genuine state (basically a $q\bar{q}$ state) which decays into two pions. Even then the Lüscher formalism, or our version of it, can be applied to obtain the ρ properties from the $\pi\pi$ phase shifts, as we are doing here.

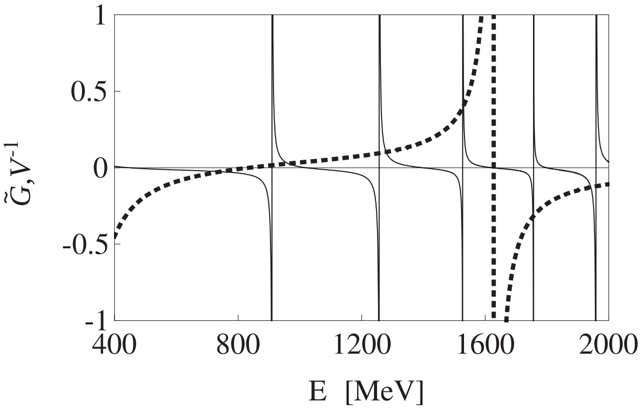

FIG. 5: The dashed curve is the $\pi\pi$ inverse potential $V_{11}(E)^{-1}$ calculated using the chiral unitary approach [41]. The solid line is $\tilde{G}$.

IV. DEPENDENCE ON THE PION MASS

In this section, we study the mass and decay width of the ρ meson using different pion masses. There has been pioneering work along these lines using effective theories in [56], evaluating the ρ self-energy with infrared regularization, but the results depend on four low energy constants that ultimately are fitted to lattice data.

We define m_π^0 to be the physical π mass, and now m_π is a free parameter. It changes from m_π^0 to $3m_\pi^0$ in our study. When changing m_π, other parameters in our previous formulae, especially the parameter f (f_π) used in Eqs. (2), can also change at the same time. The variation of f_π as a function of m_π has been calculated using the IAM in [57, 58] and it compares favorably with lattice QCD calculations [59–61]. Using the data shown in Fig. 1 of [57], and after fixing $f_\pi(m_\pi^0) = 87.4$ MeV, the value used in our previous calculation, we find the following fit:

$$f_\pi(m_\pi) = 84.4\text{MeV} + 3\text{MeV} \times \frac{m_\pi}{m_\pi^0}\,. \tag{20}$$

The coupling G_V with the vector meson dominance assumption of [62, 63] is related to f_π [64], as $G_V = f_\pi/\sqrt{2}$. We still take the value $G_V = 53$ MeV of [41] but assume it to be proportional to f_π as a function of m_π. On the other hand, the bare ρ mass, M_ρ in Eqs. (2), ofters the link of the theory to a genuine component of the ρ meson, not related to the pion cloud, and we assume it to be m_π independent.

Having all the input, we can use the same procedure to calculate the energy levels using different m_π values. We show the energy levels using $m_\pi = 1.5\ m_\pi^0$ (left), $m_\pi = 2.0\ m_\pi^0$ (middle) and $m_\pi = 2.5\ m_\pi^0$ (right) in Fig. 6. We note that the x-coordinate is expressed in units of m_π^{-1}, not $(m_\pi^0)^{-1}$.

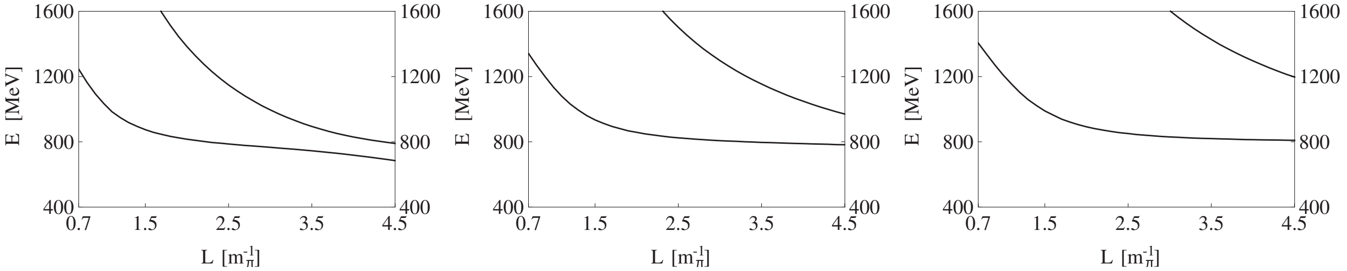

FIG. 6: Energy levels as functions of the cubic box size L. The left, middle and right figures correspond to $m_\pi = 1.5\ m_\pi^0$, $m_\pi = 2.0\ m_\pi^0$ and $m_\pi = 2.5\ m_\pi^0$, respectively.

We compare our results with the Lattice results of Ref. [18]:

Our Input and Result	Input and Result in Ref. [18]
$m_\pi = 276\text{MeV}, L = 2.75 m_\pi^{-1} = 1.96\text{fm}$	$m_\pi = 266\text{MeV}, L = 1.98\text{fm}$
$E_1 = 815\text{MeV}, E_2 = 1390\text{MeV}$	$E_1 = 812\text{MeV}, E_2 = 1431\text{MeV}$
$\delta_1 = 135.9°, \delta_2 = 175.8°$	$\delta_1 = 130.56°, \delta_2 = 146.03°$

We find that the first (lowest) energy level and the extracted phase shift from the two approaches are very similar, while those from the second energy level have small differences.

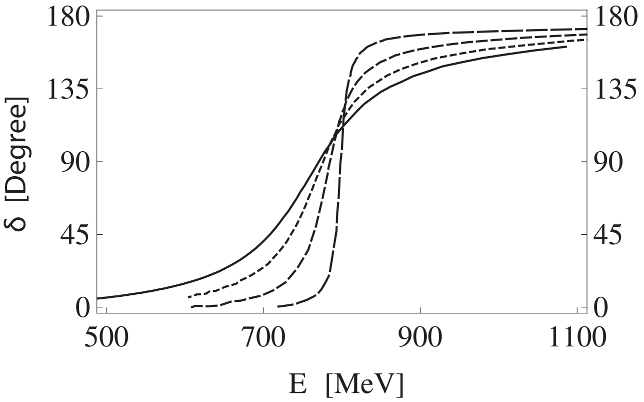

FIG. 7: The $\pi\pi$ phase shifts with different pion masses. The solid curve is obtained using physical pion mass, while the short-dashed, middle-dashed, long-dashed curves correspond to $m_\pi = 1.5\ m_\pi^0$, $m_\pi = 2.0\ m_\pi^0$ and $m_\pi = 2.5\ m_\pi^0$, respectively.

Following our previous procedure, we can use these energy levels to obtain the phase shifts. Again we only consider the first (lowest) energy level. The results are shown in Fig. 7. The solid curve is obtained using the physical pion mass, while the short-dashed, middle-dashed, long-dashed curves correspond to $m_\pi = 1.5\ m_\pi^0$, $m_\pi = 2.0\ m_\pi^0$ and $m_\pi = 2.5\ m_\pi^0$, respectively.

TABLE I: The ρ mass, coupling and decay width obtained according to Eq. (16).

m_π (m_π^0)	1.0	1.25	1.5	1.75	2.0	2.25	2.5	2.75
m_ρ (MeV)	769.6	772.8	775.7	780.0	785.0	791.3	798.6	806.6
$g_{\rho\pi\pi}$	6.79	6.56	6.32	6.10	5.92	5.62	5.46	5.25
Γ (MeV)	144	119	93.2	69.9	49.1	29.6	15.1	4.26

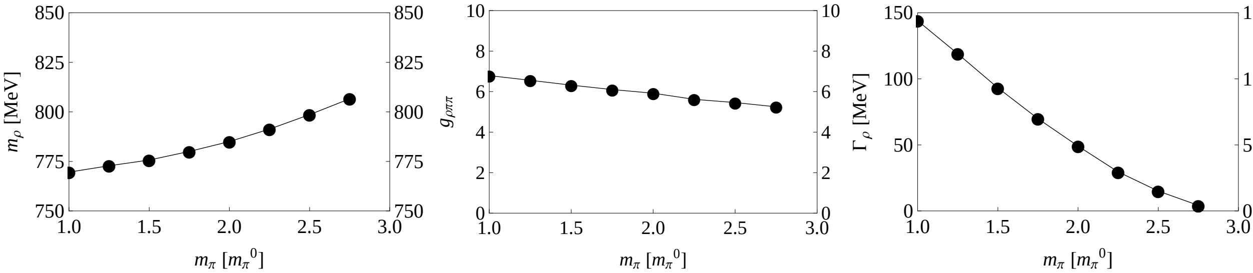

FIG. 8: The ρ mass (left), the coupling constant $g_{\rho\pi\pi}$ (middle) and the decay width Γ_ρ (right) as functions of m_π.

Using the phase shifts shown in Fig. 7, we can obtain the ρ mass (left), the coupling constant $g_{\rho\pi\pi}$ (middle) and the decay width Γ_ρ (right), which are shown in Fig. 8 as functions of m_π. We also show the numbers in Table I. Again we compare our results with the Lattice results in Ref. [18]. They use $m_\pi = 266$ MeV, and the obtained results are $m_\rho = 792 \pm 7 \pm 8$ MeV and $g_{\rho\pi\pi} = 5.13 \pm 0.20$. After correcting $g^2_{\rho\pi\pi}$ for the factor $\frac{8\pi}{6\pi}$, the obtained results in [18] are $m_\rho = 792 \pm 7 \pm 8$ MeV and $g_{\rho\pi\pi} = 5.93 \pm 0.24$ in our normalization. The obtained ρ mass $792 \pm 7 \pm 8$ MeV is in agreement, within errors, with our result $m_\rho(m_\pi = 274\text{MeV}) = 785.0$ MeV ($n = 2$ in Table I), while the obtained coupling constant $g_{\rho\pi\pi} = 5.93 \pm 0.24$ is practically identical to our result $g_{\rho\pi\pi}(m_\pi = 274\text{MeV}) = 5.92$.

V. COMPARISON WITH OF OUR RESULTS WITH THE STANDARD LÜSCHER'S APPROACH

In the Lattice QCD calculations, the Lüscher's approach is used, which is a bit different from ours as discussed in [24]. To make our analysis complete, especially for the comparison of our results with the Lattice results, in this section we show what one would get from the energy levels obtained here using the standard Lüscher's approach. It was shown in [24] that the exact form of the two meson propagator $I(q)$ of Eq. (11), where $\vec{q}$ is the integration or summation variable, could be expressed in the following form

$$\begin{aligned}\frac{1}{2\omega_1\omega_2}\frac{\omega_1+\omega_2}{E^2-(\omega_1+\omega_2)^2+i\epsilon} &= \frac{1}{2E}\frac{1}{p^2-\vec{q}^2+i\epsilon} - \frac{1}{2\omega_1\omega_2}\frac{1}{\omega_1+\omega_2+E} \\ &\quad - \frac{1}{4\omega_1\omega_2}\frac{1}{\omega_1-\omega_2-E} - \frac{1}{4\omega_1\omega_2}\frac{1}{\omega_2-\omega_1-E}\,,\end{aligned} \tag{21}$$

where $p = \lambda^{1/2}(E^2, m_\pi^2, m_\pi^2)/2E$ and $\lambda(x,y,z) = (x-y-z)^2 - 4yz$. In the standard Lüscher's approach only the first term of the right hand side of this equation is kept. This guarantees that the imaginary part of the propagator is kept exactly, but real terms (which are actually exponentially suppressed in L) are neglected. We want to show here the effect of neglecting these terms in the analysis that we have done.

We obtain Lüscher's approach using our formalism, changing $I(q)$ by the first term of Eq. (21). We use as input the energy levels which we have calculated in Sec. III using our G-function (Eqs. (8) and (10)), and then obtain the phase shifts as discussed before but using our expression for $I(q)$ or the approximate one that leads to Lüscher's approach. Since we have two sets of energy levels, for the single $\pi\pi$ channel and for the coupled channels, we take these two sets. The results are quite similar for the single and two channel cases and we show the results in Fig. 9. The left and right figures are for single channel and coupled channels "synthetic data", respectively, extracted with just the $\pi\pi$ channel analysis. We find that in the low energy region the results using the two different approaches are quite similar, while the differences become larger as the energy gets bigger. The new results with the Lüscher's approach using the single $\pi\pi$ "synthetic data" are

$$m_\rho = 786.6 \text{ MeV}\,, g_{\rho\pi\pi} = 7.66\,, \Gamma = 189 \text{ MeV}\,, \tag{22}$$

while those obtained from the coupled channels "synthetic data" are

$$m_\rho = 789.5 \text{ MeV}\,, g_{\rho\pi\pi} = 7.94\,, \Gamma = 204 \text{ MeV}\,. \tag{23}$$

We can see that there are quite some differences from using one or the other approach. One should however realize that the differences come because the phase shifts for energies around 900-1000 MeV are obtained in our case from data with L rather small, of the order of m_π^{-1} or smaller. In the work of [18] small sizes are avoided by getting data

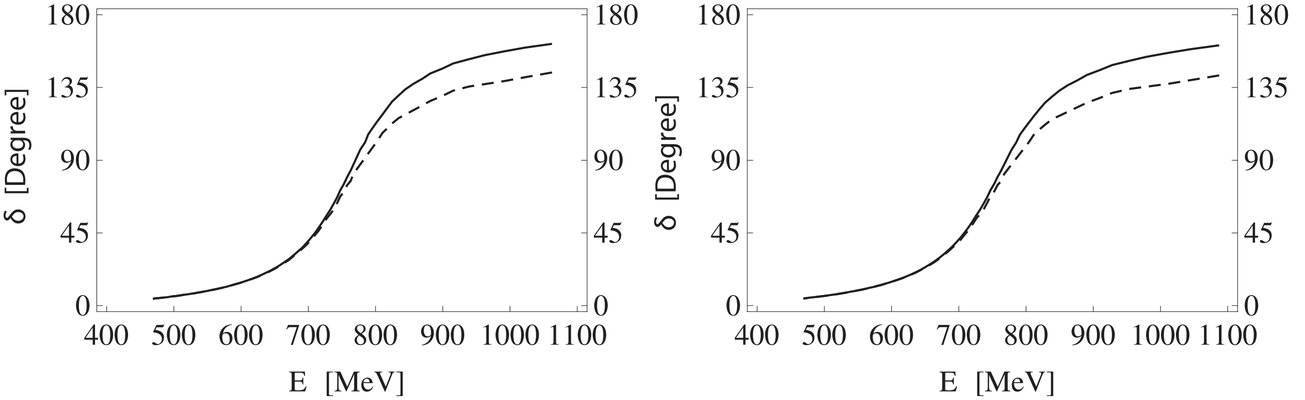

FIG. 9: The comparison between our result (solid curves) with the standard Lüscher's approach (dashed curves), respectively. The curves at the left and right hand side are extracted from the first energy level using one-channel and two-channel approach, respectively.

using instead the $\pi\pi$ system in moving frames for which the formalism is also available in [65–68], and in [39, 69] using the formalism of [24]. This avoids having to go to small values of L to get higher energies. Conversely, what we are telling here is that one could use smaller lattice sizes, with the consequent economy in the lattice calculations, but then the analysis would have to be done with our formalism, since the standard Lüscher's approach would not provide sufficient accuracy.

VI. THE INVERSE PROCESS OF GETTING PHASE SHIFTS FROM LATTICE DATA FROM TWO LEVELS.

In this section we study the inverse process of getting phase shifts from Lattice Data[24, 33, 38, 39, 55] using two levels and a parametrized potential. The method was shown to be rather efficient in [24, 33, 38, 39, 55] (see also [38] for other possible parameterizations which induce a bigger dispersion on the obtained results). The energy levels in Fig. 2 and Fig. 3 obtained in Sec III contain more information than the one that one obtains using only one level, as we have done so far. In this section we assume that they are "Lattice" inputs (synthetic data) and analyze them. We shall try to obtain the V-matrices as well as the phase shifts from these "Lattice" data. The procedure followed here also serves to get an idea of the uncertainties of the phase shifts for a given accuracy of the "lattice data".

Since we found that in the region of interest using just the $\pi\pi$ channel provides phase shifts with a high accuracy, we do the one channel analysis and obtain the V-matrix. We use the following function which accounts for a CDD pole [50]) to do the one-channel fitting:

$$V_{\pi\pi}(s) = c_1 p_\pi^2 \Big(1 + \frac{c_2 s}{c_3^2 - s}\Big) \,. \tag{24}$$

where c_1, c_2 and c_3 are three free parameters which we shall fit with the "Lattice" data shown in Fig. 2. We note that these data are calculated using the coupled channels, but, as mentioned, we find that the single $\pi\pi$ channel can already give a good enough fitting. We should mention that with this potential and the formalism of the paper we can accommodate forms of the T-matrix which are more general than just a Breit-Wigner, which is usually assumed in many Lattice calculations. Our procedure follows Refs. [24, 33]. We take five energies from the first level and five more from the second one, and we associate to them an error of 10 MeV. The following set of parameters leads to a minimum $\chi^2_{\rm min} = 0.15$:

$$c_1 = 9.2 \times 10^{-5}\mathrm{MeV}^{-2} \,,\, c_2 = 0.73 \,,\, c_3 = 843\mathrm{MeV} \,. \tag{25}$$

In Fig. 10 we show our fitting results calculated from all the possible sets of parameters having $\chi^2 < \chi^2_{\rm min} + 1$. We find that when the energy becomes larger, the error bars become larger at the same time, but the fitting is quite good. Nevertheless, we observe that the percentage in the errors of the induced phase shifts is larger than the one in the value of the energies of the box.

In the former analysis we have used the same regularization that was used in the direct problem of getting phase shifts from the chiral unitary approach. However, in a blind analysis one does not know how the G-function should be regularized. As mentioned in [24] the results of this inverse analysis do not depend on which cut off, or subtraction constant one uses in the analysis, as far as one uses the same ones to induce V from the lattice data and then later on to get the phase shifts in the infinite volume from Eq. (1). For this purpose we change the constant -2 in Eq. (8) by -1 and -3 and repeat the procedure. The results are shown in Fig. 11 and 12. As one can see, the results for the phase shifts are essentially the same, confirming once more the findings of [24].

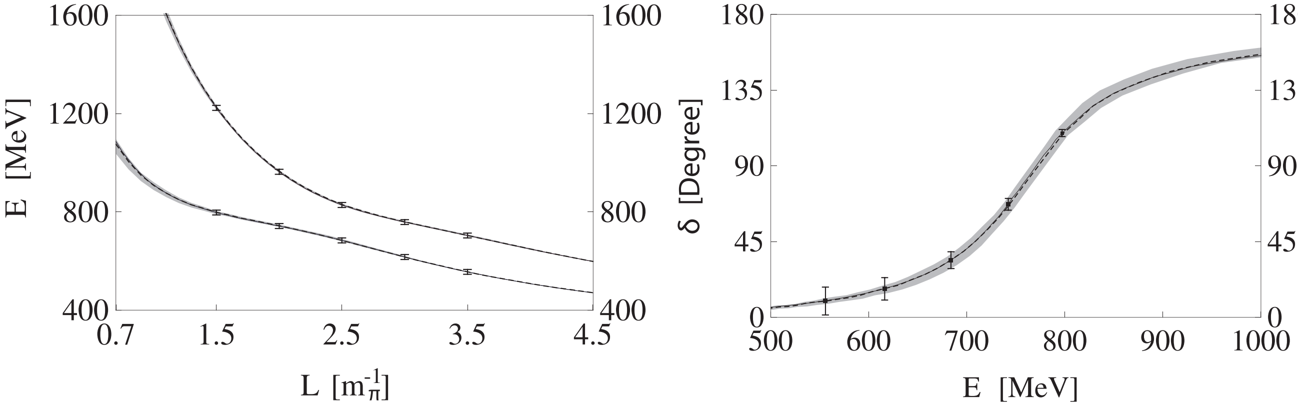

FIG. 10: Generated data points (10 MeV error, 10 points for each set). The solid curves are the orginal results, and the dashed curves (shaddy band) are the fitted results. Fits that fulfill the $\chi^2_{\rm min} + 1$ criterion are also shown in all figures (bands). The G-function of Eq. (8) is used here. The discrete points in the figure to the right are the results of the direct determination from each "data" points on the figure to the left using Eqs. (14-15) (see text).

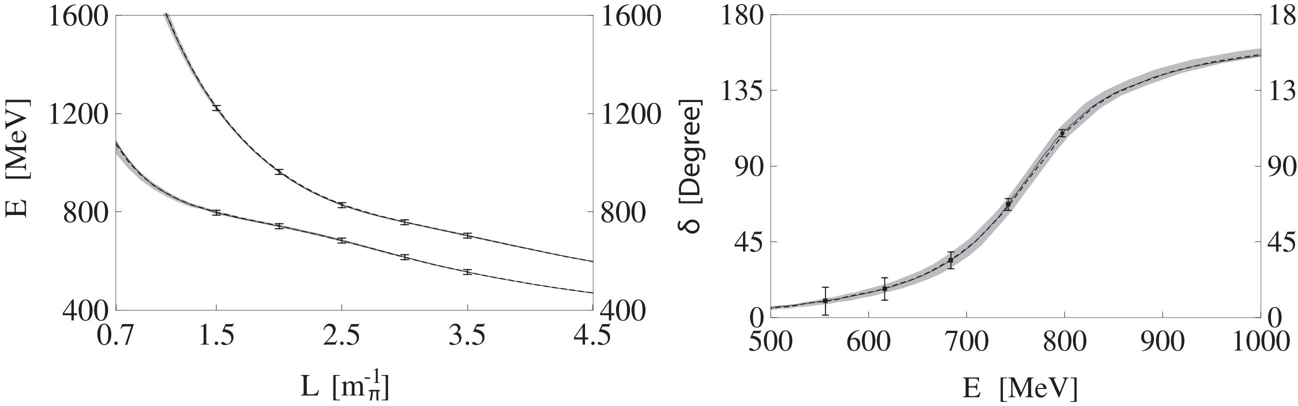

FIG. 11: Same as in Fig 10. Here we replace the constant -2 of Eq. (8) by -1.

In Figs. 10, 11 and 12 we see the band of values for the phase shifts and some discrete values with error bars. The band of values has been obtained with a fit to the synthetic data with a potential as explained before (*fit method*). The discrete points correspond to the extraction via Eqs. (14-15) of the phase shifts from each individual synthetic data of the five energies of the lower level shown on the left of the figures, with their corresponding error (*direct method*). We can see that the errors in the phase shifts are large at small energies but they become smaller as the energy increases. Yet, the overall fit to the whole set of the 10 data from two levels provide a more accurate global determination of the phase shifts than the *direct method* in the whole energy range.

VII. CONCLUSION

We have made a study of the $\pi\pi$ interaction in p-wave in a finite box using the chiral unitary approach which is very successful to provide phase shifts and the pion form factor. With this procedure we obtain discrete energies in the box as a function of L and of m_π which compare favorably with present lattice results. The second part consist of

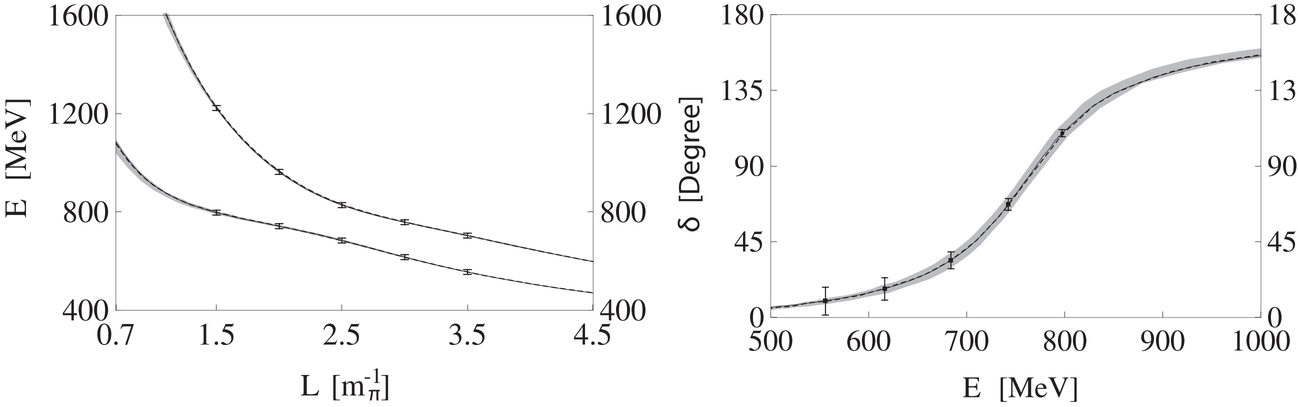

FIG. 12: Same as in Fig 10. Here we replace the constant -2 of Eq. (8) by -3.

getting the $\pi\pi$ phase shifts in infinite volume from these finite box energies for what we use our equivalent procedure to Lüscher's approach developed in [24], which improves it for small lattice sizes. We use two methods, the first one (*direct method*), valid for only one channel, produces the phase shifts without having to use an intermediate potential. The second one uses a parametrized potential and makes a fit to data. This second procedure takes advantage of the correlation among data and provides a global fit that allows one to get phase shifts for all energies and not only for the energies which are eigenvalues of the box, as in the first method, or in Lüscher's approach.

We also estimated errors induced in the phase shifts from the errors in the energies of the box. We could see that by taking a set of about 10 energies from two levels one could induce good phase shifts with reasonable errors, although we noted that the percentage of the errors in the phase shifts was larger than the one in the energies, Typically, errors of 10 MeV in the eigenenergies of the box resulted in large errors for small energies using the *direct method* but smaller errors at energies around 800 MeV. The fit method provides a better global agreement for all energies and the errors in the phase shifts, induced by the 10 MeV uncertainties in the eigenenergies of the box, are of the order of 6%.

So far we have used the centroid of the synthetic data centered at the exact curve. In actual lattice data there will also be a dispersion of the centroids. In [24] this was taken into account and a good statistical study was done. The conclusion, which we can accept also in the present case, is that taking into account a dispersion of the centroids of about 5 MeV, produces extra uncertainties in the results of maximum 50% of those produced by the 10 MeV uncertainty of the data. Hence we end with a round 10% errors in our case.

We also showed that if one uses periodic boundary conditions in the rest frame of the $\pi\pi$ system one has to use small values of the box size where the standard Lüscher approach produces too large errors. While this problem has been avoided in some lattice works by obtaining data in a $\pi\pi$ moving frame, we show that using our procedure one can go to smaller sizes with a considerable saving of the computer time in actual QCD lattice calculations. These findings can serve as a guideline for future studies of the ρ meson in these calculations, which would also allow to use pion masses closer to the physical one.

Acknowledgments

We would like to thank B. X. Sun for help in the calculations at the early stage of the problem. A careful reading and comments from U.-G. Meißner, A. Martinez Torres, M. Döring and L. Roca are much appreciated. This work is partly supported by DGICYT contract FIS2011-28853-C02-01, the Generalitat Valenciana in the program Prometeo, 2009/090, and the EU Integrated Infrastructure Initiative Hadron Physics 3 Project under Grant Agreement no. 283286, the National Natural Science Foundation of China under Grant No. 11147140, and the Scientific Research Foundation for the Returned Overseas Chinese Scholars, State Education Ministry.

[1] Y. Nakahara, M. Asakawa, T. Hatsuda, Phys. Rev. **D60** (1999) 091503.
K. Sasaki, S. Sasaki and T. Hatsuda, Phys. Lett. B **623** (2005) 208.
[2] N. Mathur, A. Alexandru, Y. Chen *et al.*, Phys. Rev. **D76** (2007) 114505.

[3] S. Basak, R. G. Edwards, G. T. Fleming *et al.*, Phys. Rev. **D76** (2007) 074504.
[4] J. Bulava, R. G. Edwards, E. Engelson *et al.*, Phys. Rev. **D82** (2010) 014507.
[5] C. Morningstar, A. Bell, J. Bulava *et al.*, AIP Conf. Proc. **1257** (2010) 779.
[6] J. Foley, J. Bulava, K. J. Juge *et al.*, AIP Conf. Proc. **1257** (2010) 789.
[7] M. G. Alford and R. L. Jaffe, Nucl. Phys. B **578** (2000) 367.
[8] T. Kunihiro, S. Muroya, A. Nakamura, C. Nonaka, M. Sekiguchi and H. Wada [SCALAR Collaboration], Phys. Rev. D **70** (2004) 034504.
[9] F. Okiharu *et al.*, arXiv:hep-ph/0507187; H. Suganuma, K. Tsumura, N. Ishii and F. Okiharu, PoS **LAT2005** (2006) 070; Prog. Theor. Phys. Suppl. **168** (2007) 168.
[10] C. McNeile and C. Michael [UKQCD Collaboration], Phys. Rev. D **74** (2006) 014508; A. Hart, C. McNeile, C. Michael and J. Pickavance [UKQCD Collaboration], Phys. Rev. D **74** (2006) 114504.
[11] H. Wada, T. Kunihiro, S. Muroya, A. Nakamura, C. Nonaka and M. Sekiguchi, Phys. Lett. B **652** (2007) 250.
[12] S. Prelovsek, C. Dawson, T. Izubuchi, K. Orginos and A. Soni, Phys. Rev. D **70** (2004) 094503; S. Prelovsek, T. Draper, C. B. Lang, M. Limmer, K. F. Liu, N. Mathur and D. Mohler, Conf. Proc. C **0908171** (2009) 508; Phys. Rev. D **82** (2010) 094507.
[13] H. -W. Lin *et al.* [Hadron Spectrum Collaboration], Phys. Rev. **D79**, 034502 (2009).
[14] C. Gattringer, C. Hagen, C. B. Lang, M. Limmer, D. Mohler, A. Schafer, Phys. Rev. **D79**, 054501 (2009).
[15] G. P. Engel *et al.* [BGR [Bern-Graz-Regensburg] Collaboration], Phys. Rev. **D82**, 034505 (2010).
[16] M. S. Mahbub, W. Kamleh, D. B. Leinweber, A. O Cais, A. G. Williams, Phys. Lett. **B693**, 351-357 (2010).
[17] R. G. Edwards, J. J. Dudek, D. G. Richards, S. J. Wallace, Phys. Rev. **D84**, 074508 (2011).
[18] C. B. Lang, D. Mohler, S. Prelovsek and M. Vidmar, Phys. Rev. D **84**, 054503 (2011).
[19] S. Prelovsek, C. B. Lang, D. Mohler and M. Vidmar, PoS **LATTICE2011**, 137 (2011).
[20] M. Lüscher, Commun. Math. Phys. **105** (1986) 153.
[21] M. Lüscher, Nucl. Phys. B **354** (1991) 531.
[22] V. Bernard, U. -G. Meissner, A. Rusetsky, Nucl. Phys. **B788**, 1-20 (2008).
[23] V. Bernard, M. Lage, U. -G. Meissner, A. Rusetsky, JHEP **0808**, 024 (2008).
[24] M. Doring, U. -G. Meissner, E. Oset and A. Rusetsky, Eur. Phys. J. A **47**, 139 (2011).
[25] X. Feng *et al.* [ETM Collaboration], PoS LAT **2010**, 104 (2010).
[26] S. Aoki *et al.* [CP-PACS Collaboration], Phys. Rev. D **76**, 094506 (2007).
[27] M. Gockeler *et al.* [QCDSF Collaboration], PoS LATTICE **2008**, 136 (2008).
[28] S. Aoki *et al.* [PACS-CS Collaboration], PoS LATTICE **2010**, 108 (2010).
[29] X. Feng, K. Jansen and D. B. Renner, Phys. Rev. D **83**, 094505 (2011).
[30] J. Frison *et al.* [Budapest-Marseille-Wuppertal Collaboration], PoS LATTICE **2010**, 139 (2010).
[31] C. McNeile *et al.* [UKQCD Collaboration], Phys. Lett. B **556**, 177 (2003).
[32] M. Doring, J. Haidenbauer, U. -G. Meissner, A. Rusetsky, Eur. Phys. J. A **47**, 163 (2011).
[33] A. Martinez Torres, L. R. Dai, C. Koren, D. Jido and E. Oset, Phys. Rev. D **85**, 014027 (2012).
[34] E. E. Kolomeitsev, M. F. M. Lutz, Phys. Lett. **B582**, 39-48 (2004).
[35] J. Hofmann, M. F. M. Lutz, Nucl. Phys. **A733**, 142-152 (2004).
[36] F. -K. Guo, P. -N. Shen, H. -C. Chiang, R. -G. Ping, B. -S. Zou, Phys. Lett. **B641**, 278-285 (2006).
[37] D. Gamermann, E. Oset, D. Strottman, M. J. Vicente Vacas, Phys. Rev. **D76**, 074016 (2007).
[38] M. Doring, U. G. Meissner, JHEP **1201**, 009 (2012).
[39] L. Roca and E. Oset, arXiv:1201.0438 [hep-lat].
[40] J. A. Oller and E. Oset, Phys. Rev. D **60**, 074023 (1999).
[41] J. A. Oller, E. Oset and J. E. Palomar, Phys. Rev. D **63**, 114009 (2001).
[42] J. Gasser and H. Leutwyler, Nucl. Phys. B **250**, 465 (1985).
[43] G. Ecker, J. Gasser, A. Pich and E. de Rafael, Nucl. Phys. B **321**, 311 (1989).
[44] A. Dobado and J. R. Pelaez, Phys. Rev. D **56**, 3057 (1997).
[45] J. A. Oller, E. Oset and J. R. Pelaez, Phys. Rev. D **59**, 074001 (1999) [Erratum-ibid. D **60**, 099906 (1999)] [Erratum-ibid. D **75**, 099903 (2007)] [hep-ph/9804209].
[46] B. Borasoy and R. Nissler, Eur. Phys. J. A **26**, 383 (2005).
[47] J. R. Pelaez, Phys. Rev. Lett. **92**, 102001 (2004).
[48] J. R. Pelaez and G. Rios, Phys. Rev. Lett. **97**, 242002 (2006).
[49] J. Nieves and E. Ruiz Arriola, Phys. Rev. D **80**, 045023 (2009).
[50] L. Castillejo, R. H. Dalitz and F. J. Dyson, Phys. Rev. **101**, 453 (1956).
[51] J. A. Oller and E. Oset, Nucl. Phys. A **620**, 438 (1997) [Erratum-ibid. A **652**, 407 (1999)] [hep-ph/9702314].
[52] J. A. Oller and U. G. Meissner, Phys. Lett. B **500**, 263 (2001).
[53] P. Estabrooks and A. D. Martin, Nucl. Phys. B **79**, 301 (1974).
[54] J. Gasser and H. Leutwyler, Nucl. Phys. B **250**, 517 (1985).
[55] J. J. Xie and E. Oset, arXiv:1201.0149 [hep-ph].
[56] P. C. Bruns and U. G. Meissner, Eur. Phys. J. C **40**, 97 (2005).
[57] J. R. Pelaez and G. Rios, Phys. Rev. D **82**, 114002 (2010).
[58] C. Hanhart, J. R. Pelaez and G. Rios, Phys. Rev. Lett. **100**, 152001 (2008).
[59] P. .Boucaud *et al.* [ETM Collaboration], Phys. Lett. B **650**, 304 (2007).
[60] S. R. Beane, T. C. Luu, K. Orginos, A. Parreno, M. J. Savage, A. Torok and A. Walker-Loud, Phys. Rev. D **77**, 014505

(2008).

[61] J. Noaki, S. Aoki, T. W. Chiu, H. Fukaya, S. Hashimoto, T. H. Hsieh, T. Kaneko and H. Matsufuru *et al.*, PoS LATTICE **2008**, 107 (2008).

[62] J.J. Sakurai, Currents and mesons (University of Chicago Press, Chicago Il 1969).

[63] M. Bando, T. Kugo and K. Yamawaki, Phys. Rept. **164**, 217 (1988).

[64] G. Ecker, J. Gasser, H. Leutwyler, A. Pich and E. de Rafael, Phys. Lett. B **223**, 425 (1989).

[65] K. Rummukainen, S. A. Gottlieb, Nucl. Phys. **B450**, 397-436 (1995).

[66] C. h. Kim, C. T. Sachrajda, S. R. Sharpe, Nucl. Phys. **B727**, 218-243 (2005).

[67] Z. Davoudi and M. J. Savage, Phys. Rev. D **84**, 114502 (2011).

[68] Z. Fu, Phys. Rev. D **85**, 014506 (2012).

[69] M. Doring, U.G. Meissner, E. Oset and A. Rusetsky, to be submitted.